Prediction of Lateral and Normal Force-Displacement Curves for Flip-chip Solder Joints

D. Wheeler, D. Josell, J.A. Warren and W.E.Wallace

National Institute of Standards and Technology,
Mettal. Div., 100 Bureau Dr., Stop 8555,
Gaithersburg, MD 20899-8555

Abstract

We present the results of experiments and modeling of flip-chip geometry solder joint shapes under shear loading. Modeling, using Surface Evolver, included development of techniques that use an applied vector force (normal and shear loading) as input to determine a vector displacement of the pads connected by the solder joint (standoff height and misalignment). Previous solutions solved the converse problem: fixed displacements used to determine required applied force. Such solutions were inconvenient for applications, where the applied force (chip weight) is known. Also, for geometric and materials studies of solder joint shapes involving multiple parameters, determining the equilibrium displacement from applied force by bracketing solutions could become computationally expensive. Measurements of solder joint standoff height and misalignment as functions of the applied force (normal and shear), solder volume and pad diameter are presented. Experiments were carried out for solder ball diameters from 0.38 mm (0.029 mm^3 volume) to 0.15 mm (0.0019 mm^3 volume) on pads of diameter 0.64 mm and 0.35 mm. Fitting of simulation to experimental results gave optimized values for the contact angle and surface tension of the solder which were consistent with measured and literature values.

Computational Modelling of Materials,
Minerals and Metals Processing
Edited by M. Cross, J.W. Evans and C. Bailey
TMS (The Minerals, Metals & Materials Society), 2001

Introduction

In packaging technology flip-chip has become an important method for attaching semiconductor devices to substrates. Generally, the chip and substrate are bumped with solder and then the chip is flipped onto the substrate and the solder reflowed to form conductive interconnects. An epoxy underfill is normally flowed between the substrate and chip to reduce the thermal fatigue on the solder joints. A flip-chip assembly is illustrated in Figure 1.

In flip-chip applications, the use of an integrated underfill/solder bump system [1, 2] removes an extra process step, namely infiltration of the underfill. However, the presence of an underfill will retard the self-alignment of the flip-chip. A first step in understanding and predicting this retardation is to develop a model to describe normal and lateral force-displacements curves when underfill material is not present. At this stage it is unclear whether static surface tension theory is sufficient to describe a complete model for flip-chip realignment even without underfill.

Possibly the most widely used code for modeling solder shape and capillary forces is Surface Evolver [3]. This code predicts the solder equilibrium shape using static surface tension theory only. Thus Surface Evolver neglects a range of relevant phenomena such as Natural and Marangoni convection as well as volume changes due to fluxing and solidification. Here, Surface Evolver is used to determine force-displacement relationships for comparison with experimental results to determine whether convection and volume changes can be ignored.

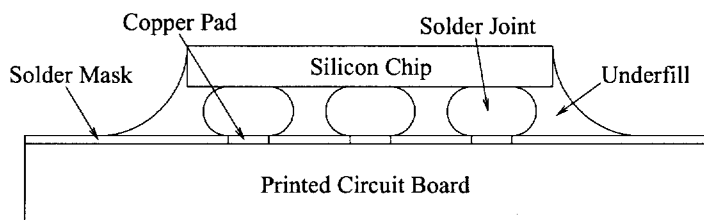

Figure 1: Flip-chip assembly with underfill, silicon chip and substrate present.

A body of work exists which has examined the misalignment of flip-chips and the similar problem of restoring forces for opto-electronic packaging using static surface tension theory alone [4, 5, 6, 7, 8]. That work did not compare experimental and modeling data for flip-chip applications at the relevant scale. Researchers have compared analytical solutions and experimental data for flip-chip oscillations on molten solder joints [9, 10]. However, interpretation of the experimental data requires an unphysical surface tension for the Pb60-Sn40 solder of 0.19 J/m [9], which is less than 50% of other published values for Pb-Sn eutectic range compositions [11, 12]. It should be noted that the solder volumes studied in reference [9] were 11 mm^3 and

16.5 mm^3, approximately 3 orders of magnitude larger than those studied here. The pad diameters were 3.81 mm, approximately 1 order of magnitude larger than those studied here.

This paper addresses the wetting behavior of solder in interconnects with the geometry of those found in the wafer-level underfill applications. Fabrication of solder joints with nominal solder volumes as small as 0.015mm^3 and pad diameters as small as 0.35mm, created under a range of shear loads, is described. Post-solidified structures are used to directly obtain force-displacement data for both normal and shear displacements. A Surface Evolver based code for flip-chip geometry is used to generate force-displacement curves for different solder volumes and pad sizes; stand-off and lateral displacements are calculated simultaneously given the normal and shear components of the applied force. Finally, the predicted and experimental results for various sized solder balls and pad radii are compared in order to evaluate the applicability of purely capillary based codes for wafer-level underfill applications, particularly at sub-300 μm pitch. The command line code, used in conjunction with Surface Evolver [3], can be found at http://www.ctcms.nist.gov/~wd15/solder/new.htm.

Experiments

Each experimental specimen is composed of eight solder joints joining copper pads arranged around a square perimeter. Flux was placed on each pad individually and solder balls were placed on the corners of the upper wafer and the edge-center pads of the lower wafer. The upper wafer was then mounted on the lower to form the flip-chip and the assembly reflowed on the hotstage. A weight was centered on the upper surface and the hotstage was tilted to the desired angle. The experimental configuration is illustrated in Figure 2. The tilt of the stage by the small angle, ϕ_{tilt}, results in normal and lateral forces where the normal force is given by,

$$F_z = \frac{mg}{n_{pads}} \cos \phi_{tilt} \tag{1}$$

and the lateral force is given by,

$$F_x = \frac{mg}{n_{pads}} \sin \phi_{tilt} \tag{2}$$

where g, n_{pads} and m are the acceleration due to gravity, the number of pads and the weight of the applied mass, respectively. After this process the stage is quenched with the specimen still subject to the shear load. The specimen is then mounted in epoxy, cross-sectioned and the displacements are measured. In order to model the data, independent values were required for the contact angle on the silicon wafers. These were obtained from direct contact angle measurements. The contact angle on

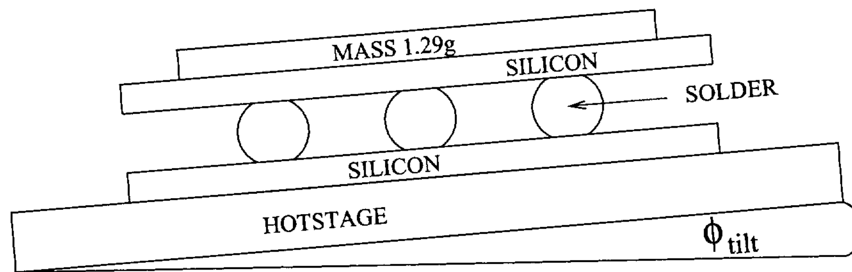

Figure 2: Schematic of the experimental configuration. Eight copper pads, each 5 μm thick with a 30 nm Ti intermediate layer on silicon wafer. Two such wafers, with a solder ball between each corresponding pair of pads, were sandwiched together to make each specimen. The pads were all either 0.64 mm or 0.35 mm in diameter. Spacing between pad centers was 5 mm.

Si was found to be 149 ± 3° (2σ uncertainty) and between $2 - 5^o$ on the copper pad. The solder used in these experiments had a eutectic composition (Sn63-Pb37). It came in the form of solder balls with nominal diameters of 0.381, 0.254, 0.229 and 0.152mm. Stated uncertainties were $\pm 25\mu$m. These nominal diameters correspond to volumes of 0.232, 0.069, 0.048 and 0.015 mm^3, respectively. Further details of the experiments are available [13].

The results of all experiments are summarized in Figures 3 to 6. Each plot shows the dependence of the lateral offset and the stand-off of the solder joint on the applied shear force. Figures 3 and 4 summarize the results for pad diameter 0.64 mm and nominal solder volumes 0.232 and 0.069 mm^3. Figures 5 and 6 summarize the results for the 0.35 mm pad diameter and nominal solder volumes 0.048 and 0.015 mm^3. The best fit Evolver generated force-displacement curves are also included in all four figures. The same best fit values of the parameters, (θ_{Si} =150° and γ=0.4 N/m^2), discussed in the modeling section of this paper, were used for all four curves. In Figure 3, the kink in the lateral offset is caused by a portion of the triple line (the curve where the solder, underlying substrate or pad and the vapor meet) moving off of the pad and starting to wet the silicon. This occurs when the contact angle at that location reaches θ_{Si}. This can be contrasted with the results in Figure 4 where the triple line is entirely on the pad perimeter and Figure 5 where a portion of the triple line lies on the substrate for all shear force values.

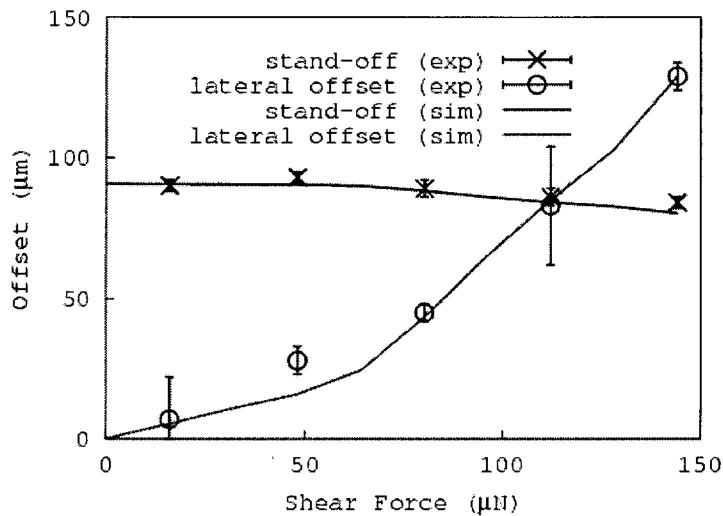

Figure 3: Experimental and best fit simulation for 0.381 mm solder balls. Experimental data and best fit modeling results are shown for both the stand off and lateral offsets as functions of the shear force (normal force varies by less than 0.5% over the full range). The triple line remains entirely on the perimeter of the pad only for shear forces smaller theta 60μN. For larger shear forces a portion of the triple line is on the substrate.

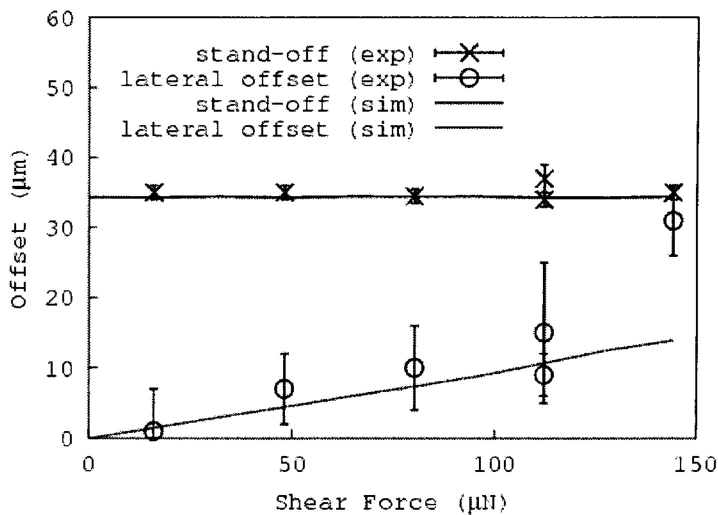

Figure 4: Experimental and best fit simulation for 0.254 mm solder balls . Experimental data and best fit modeling results are shown for both the stand-off and lateral offsets as functions of the shear force (normal force varies by less than 0.5% over the full range). The triple line lies on the pad perimeter for the range of shear forces shown.

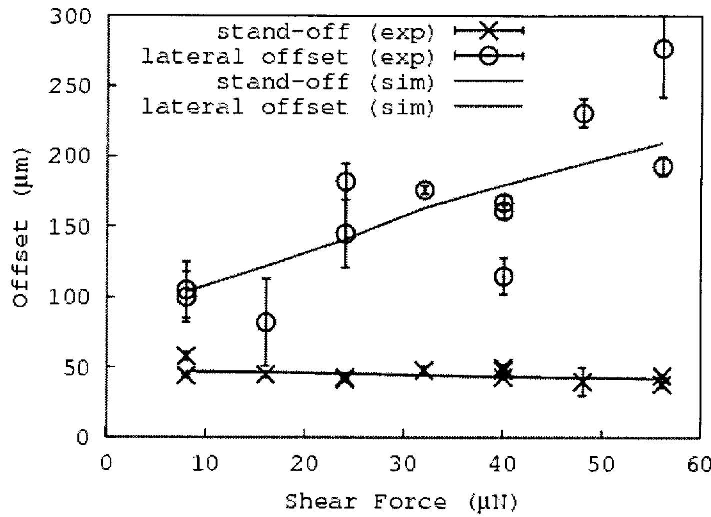

Figure 5: Experimental and best fit simulation for 0.229 mm solder balls . Experimental data and best fit modeling results are shown for both the stand off and lateral offsets as functions of the shear force (normal force varies by less than 0.5% over the full range). The triple line lies on the substrate for the range of shear forces shown.

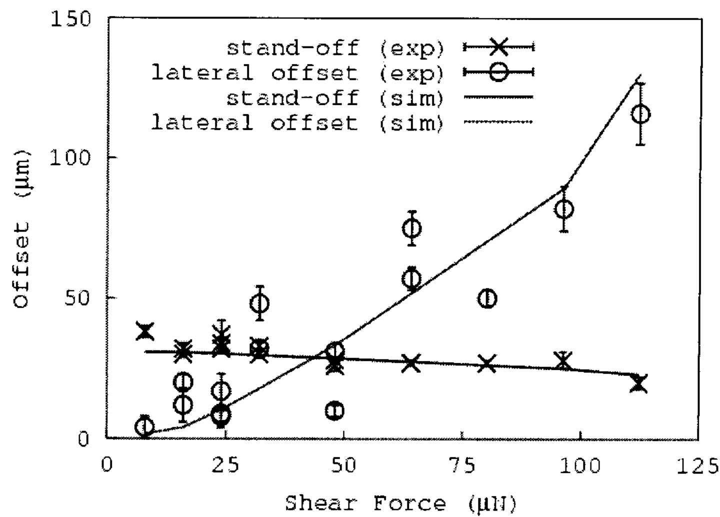

Figure 6: Experimental and best fit simulation for 0.152 mm solder balls. The triple line wets the substrate at a shear force of 25 μN.

Modeling

Prediction of force-displacement curves for array type interconnects has until now been confined to predicting the force given a displacement, e.g. [14]. Unfortunately, the normal and lateral displacements are interdependent, each depending on both the normal and lateral components of the applied force. In theory, equilibrium displacements can be obtained from fixed displacement models using a bracketing technique for the energy. However this is time-consuming, requiring many simulations for each data point, making it especially cumbersome for studies involving a range of geometric and material parameters.

The Evolver solution procedure does not require user interaction and involves using an energy bracket at each stage of the mesh refinement to move the displacement parameters. With the understanding that the pad is fully wetted, the total energy for the solder configuration is given by,

$$E = F_x x_0 + F_z h + \int_S \gamma dS - 2\pi r_{pad}^2 \gamma \cos\theta_{pad} - \gamma \cos\theta_{Si} \int_0^{2\pi} (r_{tl}^2(\phi) - r_{pad}^2) d\phi \tag{3}$$

where F_x, x_0, F_z, h, S, γ, r_{pad}, θ_{pad}, θ_{Si}, r_{tl} and ϕ represents the lateral force, lateral displacement, normal force, stand-off height, solder surface area, surface tension, pad radius, pad contact angle, silicon wetting angle, distance from center of pad to triple line and radial angle. The last two terms in Equation (3) are the wetting energies of the areas on the upper and lower wetted surfaces (allowing their facets to be otherwise omitted). While $\theta_{Si} > \theta > \theta_{pad}$, the local triple point remains on the pad perimeter. If $\theta_{Si} < \theta$, then the triple point wets onto the silicon. The condition $\theta_{pad} > \theta$ never occurred during either the experiments or the simulations. (i.e. no de-wetting of the pad)

Table I shows the results of an analysis obtained by allowing the surface tension, γ, and the contact angle on the silicon, θ_{Si}, to be simultaneous fitting parameters for all the data from the four geometries. Every experimental lateral offset and stand-off data point is included. Experimental uncertainty values for each data point were used for normalizing. The best fit is obtained for values of $\theta_{Si} = 150^o$ and γ=0.4 N/m^2, although a continuum of values with increasing γ_0 and decreasing θ_{Si} also fits the data reasonably well. The consistency of the optimal angle and the experimentally obtained value of 149° already noted is significant, as is the fact that the associated optimal value for γ is also reasonable.

In order to understand the trends in the fit, the following should be understood. First, fitting of data where the triple line is fully on the perimeter (i.e., the solder does not wet the substrate) will give a quality of fit that is independent of θ_{Si}. Therefore, in the analysis, this subset of the experimental data only affects the selection of the optimal value of γ. This data corresponds to low shear stresses (less than the value for the kink indicating initial wetting of the substrate) and/or small solder volume.

Table I: Least squares fitting of all experimental data.

χ^2	$\theta_{Si} = 140^o$	150°	160°
γ=0.3 N/m^2	499.8	212.3	93.5
0.35	159.0	36.1	9.3
0.4	35.4	**6.7**	13.8
0.45	8.6	17.0	32.8

The shear force at which the kink occurs depends on both θ_{Si} and γ. Also, once the triple line moves onto the substrate, the slope of the force-displacement (lateral offset) curve depends on both γ and θ_{Si} as a result of the Young-Laplace equation.

The optimization of data involved minimizing the deviation of experimental data and predictions from the Evolver code. This included weighting each data point by the experimental uncertainty associated with that particular measurement (see Figures 3 to 6). All experimental data, both lateral offset and stand-off, from all four solder ball sizes were used. An experimentally measured average volume, rather than the nominal value, was used for modeling the force-displacement curves for the smallest solder ball [13].

Conclusion

This paper presented the wetting behavior of solder in interconnects with the geometry of those found in the wafer-level underfill applications. A Surface Evolver based code for flip-chip geometry was used to generate force-displacement curves for different solder volumes and pad sizes. Comparison of the experimental results and those obtained from Surface Evolver are consistent.

The motivation of this study was to assess the validity of using only static surface tension theory for use in understanding flip-chip misalignment in order to ascertain whether realignment will occur with underfill present at the reflow stage. The qualitative and quantitative agreement for the substrate wetting and optimized parameter values (γ, θ_{Si}) suggest that static theory is a good approximation to predict the behavior in these experiments. The value of θ_{Si} is near the independent measured value and γ is consistent with values from the literature. It is therefore evident that, for the dimensions and materials used in this study, only capillary and gravitational forces are required to accurately predict solder joint stand-off heights and lateral offsets given applied shear and normal forces.

Finally, a novel computer code that permits solder joint displacements to be determined given applied forces (rather then the converse), was developed in this effort. It has been shown to be accurate, as well as more convenient than codes that solve for

forces given displacements.

References

[1] C.D. Johnson and D.F. Baldwin. In *Proceedings of the 1999 Electronic Components and Technology Conference*, page 950, 1999.

[2] C.D. Johnson and D.F. Baldwin. In *1999 International Symposium on Advanced Packaging Materials*, page 73, 1999.

[3] K.A. Brakke. *Surface Evolver.* The Geometry Centre, 1300 South Second Street, Minneapolis, MN 55454, 2.00 edition, April 1996. available from http://www.geom.umn.edu.

[4] S.E. Deering and J. Szekeley. Mathematical-modeling of alternative pad designs in flip-chip soldering processes. *Journal of electronic packaging*, 23(12):1325–1334, dec 1994.

[5] W. Lin, S.K. Patra, and Y.C. Lee. Design of solder joints for self-alligned optoelectronic assemblies. *IEEE Transactions On Components, Packaging and Manufacturing Technology - Part B*, 18(3):543–551, August 1995.

[6] S.M. Heinrich, M. Schaefer, S.A. Schroeder, and P.S. Lee. Prediction of solder joint geometries in array-type interconnects. *Journal of Electronic Packaging*, 118(3):114–121, 1996.

[7] T.S. Lee, T.P. Choi, and C.D. Yoo. Finite element modeling of three-dimensional solder joint geometry in smt. *Journal of Engineering Packaging*, 119:119–126, 1997.

[8] K.F. Harsh, B. Su, W. Zhang, V.M. Bright, and Y.C. Lee. The realisation and design considerations of a flip-chip integrated mems tunable capacitor. *Sensors and Actuators - A Physical*, 80:108–118, 2000.

[9] M. Landy, S.K. Patra, and Y.C. Lee. In *Manufacturing Processes and Materials Challenges in Microelectronic Packaging*, page 49. AMD -131/EEP - 1, 1991.

[10] N. van Veen. Analytical derivation of the self-alignment motion of flip chip soldered components. *Journal of Electronic Packaging*, 121(2):116–121, 1999.

[11] K.W. Moon, W.J. Boettinger, M.E. Williams, et al. Dynamic aspects of wetting balance tests. *Transactions of the ASME*, 118:174–183, 1996.

[12] J.Y. Park, C.S. Kang, and J.P. Jung. The analysis of the withdrawal force curve of the wetting curve using 63sn-37pb and 96.5sn-3.5ag eutectic solders. *Journal of Electronic Materials*, 28(11):1256–1262, 1999.

[13] D. Josell, W. Wallace, J.A. Warren, and D. Wheeler. Misaligned flip-chip solder joints: Prediction and experimental determination of lateral and normal force-displacement curves. 2001.

[14] T.B. Thompson, G. Subbarayan, R. James, and F.P. Renken. private communication.